Stripping Voltammetry of Cu Overlayers Deposited on Self-Assembled Monolayers: Field Emission of Electrons through A Phenylene Ethynylene Oligomer

M. S. Doescher, J. M. Tour, A. M. Rawlett, and M. L. Myrick*

Department of Chemistry and Biochemistry, University of South Carolina, Columbia, South Carolina 29208

Received: March 7, 2000

Copper overlayers were formed on electrodes coated with self-assembled monolayers (SAMs) of a molecular wire candidate, 1-thio-4-[4′-[(4′-thio)phenylethynyl]-1′-ethynyl]-2′,5′-(diethyl)phenylbenzene (TTEB), by electrochemical reduction of copper ions and by physical vapor deposition. Anodic stripping voltammetry of copper was employed to study the electrochemical and electron transport properties of SAMs of these molecules. Electrochemical copper deposition revealed that SAMs of TTEB passivate the electrode to electrochemistry in a manner similar to alkanethiols. Migration of copper ions trapped within the TTEB SAM after copper oxidation was also observed. Reduction of the solvent prevented the application of a sufficient potential to deposit copper by conduction through the TTEB SAM, so evaporation of copper metal was employed to coat the entire electrode. Anodic stripping voltammetry first removed the metal from defect sites, leaving behind copper islands connected to the gold by TTEB molecules. At higher potentials the copper islands were oxidized via electron transport through the TTEB SAM. A barrier height of 1.17 eV to charge injection was calculated from the tunneling current and overpotential by a Fowler−Nordheim-type analysis. Tunneling currents in TTEB molecules with metal contacts were found to be dominated by hole transport.

Introduction

Recent studies have investigated the potential of single molecules or small groups of molecules to perform the functions of common electronic components.[1−3] The simplest electronic component is the wire; it allows a current of electrons to flow through it due to a potential difference between the ends of the wire. Many proposed molecular wires consist of highly conjugated rigid organic oligomers because of the extended electronic wave functions possible in conjugated π systems. Testing the conductivity of these conjugated oligomers is very important to the development of molecular electronics. High conductivity in macroscopic systems is either due to high densities of charge carriers, as in copper, or high charge carrier mobility, as in graphite. Graphite has a conjugated electronic structure similar to those of some proposed molecular wires, which suggests that they may also be good conductors. However, measuring the charge transport through a molecular wire is challenging. Due to the very small size of molecules, traditional methods to measure conductivity will not work and researchers must devise strategies to investigate this property for individual molecules.

One clever technique employed by Weiss and co-workers[4] was to allow sulfur-terminated conjugated oligomers to randomly replace alkanethiol molecules in a self-assembled monolayer (SAM)[5] and use alternating current scanning tunneling microscopy to observe the molecules and measure an apparent tunneling barrier height. From their measurements they inferred that the conjugated oligomer exhibited a greater conductivity than dodecanethiol (DT). A second, more direct measurement technique was used by Reed et al.[6] In Reed's work, molecules of 1,4-dithiobenzene were allowed to self-assemble between the Au point contacts of a mechanical break junction. However, high electric fields can produce currents due to field emission that mimic conductance through a molecular wire. In ref 6, for example, currents over 0.2 μA are passed through an organic wire under an applied voltage of 5 V. With an estimated contact separation of 8 Å, the applied field greater than 6 GV/m can induce a substantial field emission. Our own laboratory has reported plasma atomic emission from alkanethiol-coated Au samples subjected to 5 V pulses with an STM.[7−9] Under such conditions, much of the power dissipation is not across the desired sample.[10,11]

Our laboratory has previously explored the synthesis of nanoscale wires[12] and single-molecule lithography[13] by electrochemical methods. Electrochemistry also provides an alternative method for measuring conductivity across molecules. Most electrode processes are limited by diffusion rates in solution and are not directly applicable to molecular conductivity measurements. Anodic stripping voltammetry[14] (ASV), however, is an electrochemical technique in which a metal deposit is rapidly oxidized from an electrode surface with a rate that is limited only by electron transfer to or from the metal. We have explored anodic stripping voltammetry (ASV) as a tool for investigating conductivity in molecular wires and developed a technique for measuring electron transport through these conjugated organic oligomers with low current densities.

In this report, we have explored the deposition and stripping of Cu metal on Au, on SAMs of DT, and on SAMs of 1-thio-4-[4′-[(4′-thio)phenylethynyl]-1′-ethynyl]-2′,5′-(diethyl)phenylbenzene (TTEB), which is a candidate molecular wire. Both electrochemical and vapor deposition methods were used to form Cu overlayers. Our results indicate that TTEB acts as an insulator to electrochemical processes except under extreme conditions of electric field strength (>400 MV/m). Our measurements are interpreted to mean that conduction through TTEB is limited by the rate of hole injection due to a 1.17 eV barrier to charge injection that exists between the Au surface and the TTEB highest occupied molecular orbital (HOMO).

10.1021/jp0008795 CCC: $20.00
Published on Web 12/09/2000

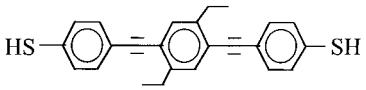

Figure 1. 1-Thio-4-[4′-[(4′-thio)phenylethynyl]-1′-ethynyl]-2′,5′-(diethyl)phenylbenzene, a molecular wire candidate.

Experimental Section

Ethanol (Aaper), tetrahydrofuran (EM Science), dodecanethiol (Aldrich), sulfuric acid (Fisher Scientific), hydrogen peroxide (Fisher Scientific), ferrocyanide (Fisher Scientific), and copper sulfate (Mallinckrodt AR) were reagent-grade and were used without further purification. Aqueous solutions were prepared with distilled, deionized water. Conjugated oligomers of 1-thio-4-[4′-[(4′-thio)phenylethynyl]-1′-ethynyl]-2′,5′-(diethyl)phenylbenzene (TTEB, Figure 1) were received from the group of J. M. Tour (Rice University) and were used without further purification.

Au working electrodes with an area of 0.02 cm^2 were purchased from BAS. They were prepared by polishing with alumina particles (Buehler) down to the 0.05 μm size. Following the polishing step, the electrodes were cleaned for 30 s in piranha solution (3:7 ratio of 30% H_2O_2:H_2SO_4) (use extreme caution when handling piranha solution) and rinsed with deionized distilled water.

The Au electrodes were coated with monolayers of TTEB by immersion of the electrode for at least 24 h in a solution of 10^{-5} M TTEB in tetrahydrofuran. Upon removal from the deposition solution, the electrode was rinsed with tetrahydrofuran. TTEB deposition occurred under argon in an inert atmosphere drybox (Vacuum Atmospheres).[5]

DT deposition also occurred under argon in an inert atmosphere drybox. The Au electrodes were coated with monolayers of DT by immersion of the electrode for at least 40 min in a solution of 0.4 mM DT in ethanol. Upon removal from the deposition solution, the electrode was rinsed with ethanol.[5]

Electrochemical data were collected by use of an EG&G Princeton Applied Research Model 263 potentiostat under computer control with a standard electrochemical cell, a saturated calomel electrode (SCE), and a platinum wire counterelectrode. All potentials are reported vs the SCE reference. Electrochemistry was performed in quiescent aqueous 1 M H_2SO_4 solutions, degassed with nitrogen, at a scan rate of 10 mV/s.[15,16]

Formation of a Cu overlayer occurred by physical vapor deposition (Mathis) in a vacuum chamber (Varian) at an approximate base pressure of 10^{-5} Torr.

Scanning electron microscopy (SEM) was done on a Hitachi S-2500 scanning electron microscope. Energy-dispersive X-ray spectroscopy (Gresham) was used to determine the elemental composition of observed features.

Results and Discussion

SAM Formation with TTEB. DT forms a SAM on Au surfaces that effectively passivates the Au surface to electrochemical processes in solution.[5] Cyclic voltammetry of ferrocyanide on DT-coated Au electrodes shows that the surface is 99% passivated, with a small residual current due to pinhole defects.[17]

TTEB is similar to other SAM-forming molecules reported in the literature.[2] To confirm that TTEB forms stable SAMs, we performed cyclic voltammetry of ferrocyanide. Figure 2 shows the first and second cyclic voltammograms (CVs) of ferrocyanide at a TTEB-coated Au electrode. The first CV (curve A in the figure) shows a lower ferrocyanide redox current than the corresponding bare Au electrode (not shown), from which we infer the presence of a defective TTEB SAM. The first CV also shows irreversible TTEB oxidation, which appears as a sharp peak at 1.4 V indicative of TTEB desorption. This peak overlaps and obscures the oxidation of the Au electrode. The magnitude of the charge passed during this oxidation is consistent with monolayer coverage. On the reverse sweep, Au oxide stripping is observed at 0.9 V. The second CV (curve B in Figure 2) shows a ferrocyanide oxidation process that is sharper and increased in magnitude, which is consistent with loss of the monolayer. Also, TTEB oxidation is not observed in the second CV.

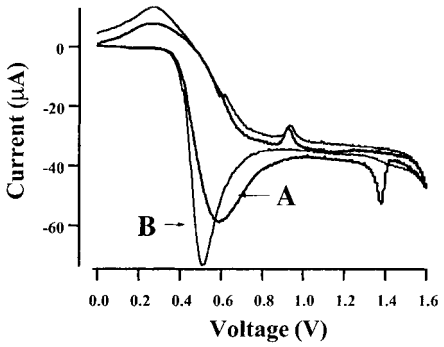

Figure 2. Cyclic voltammogram of ferrocyanide at a TTEB SAM-coated gold electrode: first (A) and second (B) scans.

ASV at Coated and Uncoated Au Electrodes. Deposition of Cu on insulating alkanethiol films has been previously reported.[17] If TTEB is conductive, the reaction of Cu on a TTEB SAM-coated electrode may be different from its behavior on more insulating SAMs. For this reason we measured the voltammetry of Cu deposition and stripping with (A) a bare Au electrode, (B) a DT monolayer, and (C) a TTEB monolayer (Figure 3). For reference, the voltammogram on uncoated Au shows Cu deposition at potentials less than 0.0 V and stripping at more positive potentials (Figure 3A).

As is found for the reaction of ferrocyanide described above, the DT SAM reduces the Cu reduction rate from that on bare Au by about 99%. Metal deposition on the DT-passivated Au electrode is known to occur at pinhole defects in the SAM where the Au surface is exposed. The onset of Cu reduction at the DT-coated electrode is shifted to more negative potentials relative to the bare Au electrode, because Cu ions require an overpotential for reduction at the defect sites (Figure 3B).[17]

The defects present in the TTEB SAMs show the same characteristic shift in deposition potential, deposition curve shape, and stripping peak (Figure 3C) observed for those in the DT SAMs. A new peak appears at 0.3 V, which, as we explain below, is likely a migration current due to expulsion of Cu ions trapped in the TTEB monolayer following oxidation of the metal overlayer.

Cu Ion Migration. To determine the origin of the +0.3 V peak, a series of voltammograms cycling between Cu deposition and stripping potentials on a TTEB-coated Au electrode was acquired in which the potential was never swept above +0.2 V (Figure 4). As the scan was repeated, a small reduction peak appears at −0.1 V and increases in magnitude with scan number. This is the same potential at which Cu deposition occurs on the bare Au electrode, and we assign this peak as a rereduction of Cu ions trapped within the SAM during the previous oxidation−reduction cycle. The trapped Cu ions do not require the overpotential for reduction in pinhole defects and so react at the same potential as Cu ions on the uncoated Au electrode.

Following electrode cycling as in Figure 4, the Cu being

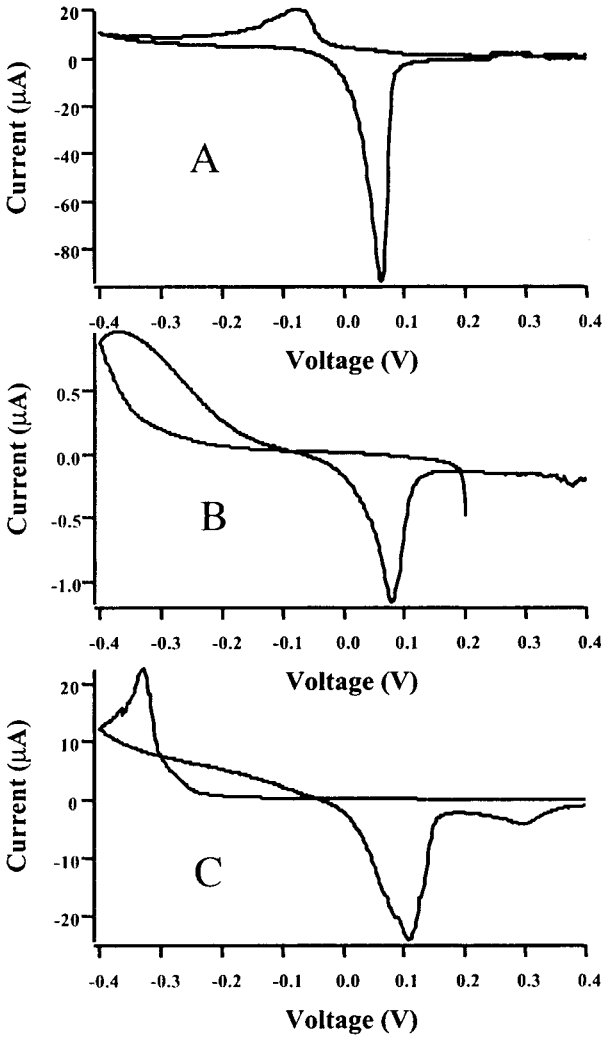

Figure 3. ASV of copper (A) at a bare gold electrode, (B) at a DT SAM-coated gold electrode, and (C) at a TTEB SAM-coated gold electrode.

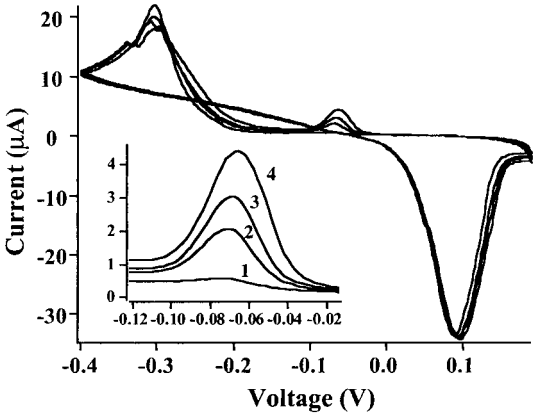

Figure 4. Sequential ASV scans of copper at a TTEB SAM-coated gold electrode.

rereduced at −0.1 V builds in concentration. When the potential of the electrode is then swept in the positive direction, a stronger migration peak at 0.3 V (Figure 5A) is observed. The very next scan shown in Figure 5B shows that the reduction peak at −0.1 is not present, indicating all of the trapped Cu has been removed from the layer. Further evidence is obtained by observing that the magnitude of the migration peak in the second CV is reduced. This is because fewer Cu ions are trapped in the layer after only a single cycle of Cu stripping.

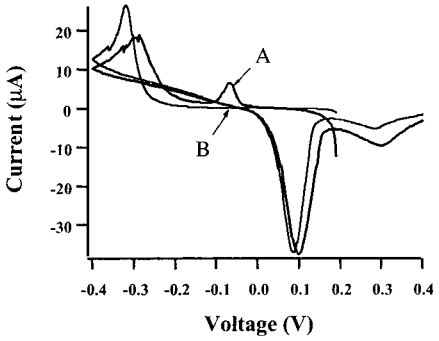

Figure 5. ASV of copper at a TTEB SAM-coated gold electrode: (A) subjected to sequential ASV scanning at potentials less than 0.2 and (B) same electrode scanned immediately after scan A is complete.

A final piece of evidence for the nature of this +0.3 V peak is obtained from voltammetry on a DT SAM that has been damaged by oxidation of the underlying Au.[17] Cu ASV on these disordered DT layers shows the same peak observed in Figure 3C. DT is known to form better SAMs than TTEB on the basis of electrochemical passivation properties. Once disrupted by oxidation, however, the DT SAM is far less passivating. The presence of the same peak on electrodes covered with different SAMs suggests the peak is not related to the chemical identity of the SAM-forming molecules but is related instead to the organization of the films.

Except for the presence of the +0.3 V migration peak, there is little difference between Figure 3 panels B and C. TTEB SAMs appear to behave similarly to DT SAMs on Au electrodes: they passivate the electrode (although not as effectively as DT) and behave as insulators. Figure 3 provides no evidence for oxidation of a metal overlayer by electron conduction through TTEB. There are two possible explanations for this observation. The first is that no Cu is ever reduced atop the TTEB layer by electrochemistry, and deposition only occurs near defects. The second is that although Cu is reduced and deposited atop the TTEB layer, the TTEB prevents its reoxidation. The first scenario seems most likely since the most negative potential we can apply to the electrode is limited by the electrochemical window of our solvent. This means we may not have been able to apply a sufficient overpotential to reduce Cu through the TTEB SAM anywhere except at defects.

To ensure that a layer of Cu was deposited on even the defect-free portions of the SAMs, SAM-coated electrodes were coated with Cu by thermal evaporation.

ASV of Vapor-Deposited Cu. Figure 6 shows the stripping voltammetry of vapor-deposited Cu on a DT SAM. The very large peak at 0.1 V is due to Cu metal oxidation though pinhole defects in the DT SAM where the Cu metal is in contact with the Au electrode. Also visible in the figure is the oxidation of Au at 1.2 V and the Au oxide stripping peak at 0.9 V. At the potential limits imposed by the solvent window in these experiments, no oxidation of DT is observed and no additional redox processes are observed. However, when the electrode is viewed under a microscope following anodic stripping of the vapor-deposited Cu film, Cu islands covering the entire surface are still observed.

Results for ASV of an evaporated Cu film at a TTEB-coated Au electrode (Figure 7) are similar to those at a DT-coated Au electrode, with a major stripping peak at +0.1 V for Cu oxidation at defects. However, new peaks appear at 1.2 and 1.4 V for TTEB-coated electrodes. The peak at +1.4 V observed in Figure 7 is due to the oxidation and desorption of TTEB from the electrode surface, similar to that observed in Figure 2.

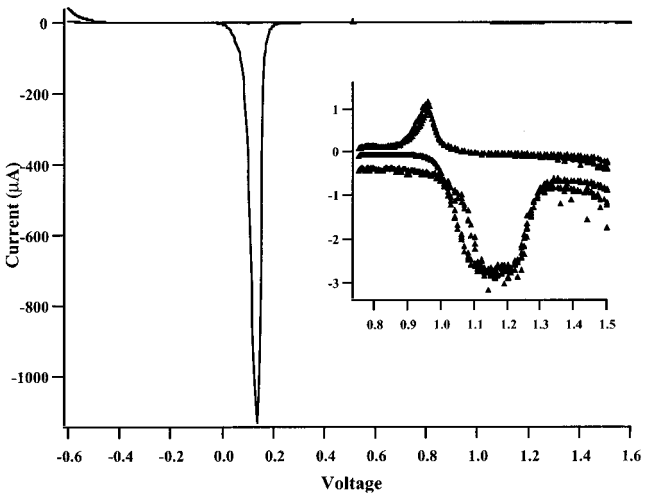

Figure 6. Stripping voltammetry of an evaporated copper overlayer on a DT SAM-coated gold electrode.

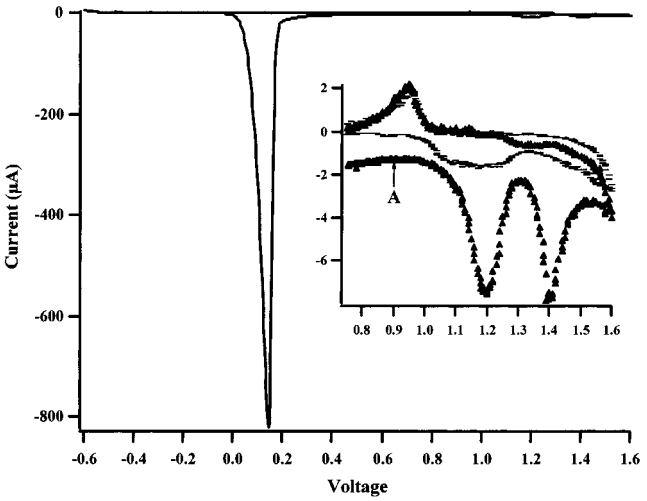

Figure 7. Stripping voltammetry of an evaporated copper overlayer on a TTEB SAM-coated gold electrode. Triangles represent the first scan while dashes represent the second scan. The point A marks the potential at which an electrode was removed from the electrochemical cell and imaged with SEM.

The new peak at +1.2 V is assigned, as explained below, as oxidation of Cu islands on the electrode face that are isolated from the Au electrode surface by defect-free domains of the TTEB SAM. The second scan shows the oxidation of Au not visible on the first scan due to the presence of the larger peak at 1.2.

To show that Cu islands remain on the electrode surface following the anodic stripping of most Cu at +0.1 V, an electrode was swept to the potential marked A in Figure 7. The electrode was then removed, rinsed, and analyzed by scanning electron microscopy. SEM (Figure 8) reveals islands on the surface that are identified as Cu by energy-dispersive X-ray spectroscopy. We interpret these islands as sitting atop ordered TTEB domains that are not normally covered with Cu by electrochemical reduction at defects.

SEM of electrode surfaces that have been swept past the +1.2 V peak in Figure 7 show that these remaining Cu islands have been stripped. The +1.2 V peak is thus assigned as being due to oxidation of Cu by charge transport through the ordered TTEB domains.

Cu is oxidized when its potential exceeds the standard potential for Cu oxidation at approximately 0.1 V. We can

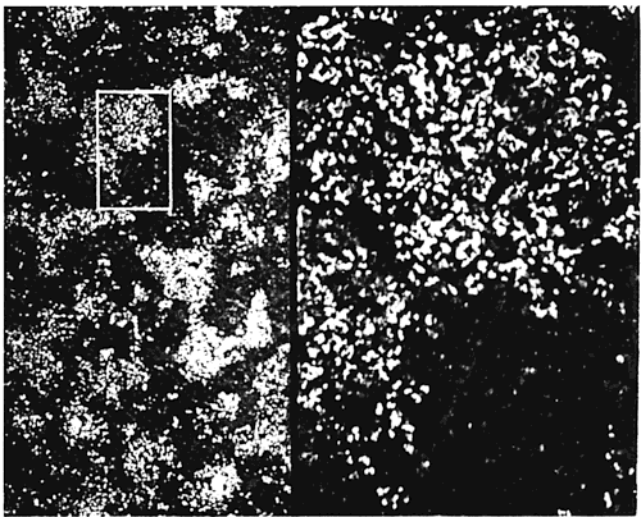

Figure 8. Scanning electron microscope image of the a gold electrode subjected to stripping voltametry of an evaporated copper overlayer on top of a TTEB SAM. The white spots are copper islands. The rectangle is 24 by 40 μm.

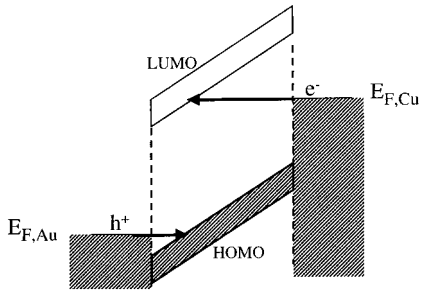

Figure 9. Schematic band diagram showing a TTEB SAM connecting a Cu overlayer to a Au electrode.

therefore take the potential of the Cu islands atop the TTEB layer during oxidation as being equal to the standard potential for Cu oxidation. The potential measured in our experiments at which that peak is observed (+1.2 V) is the potential of the Au electrode on the opposite side of the TTEB layer. The difference between the Cu standard oxidation potential and the potential at the surface of the Au electrode, 1.1 V, is therefore the voltage dropped across the TTEB SAM. This is the overpotential required to see any measurable current flow through the TTEB monolayer. Using the SAM thickness, 25.2 Å,[2] we calculate an effective electric field strength in the SAM of approximately 450 MV/m.

An electric field strength of this magnitude suggests an electron tunneling model is appropriate for interpreting electron transport through TTEB SAMs. A tunneling model implies the existence of an energy barrier to electron tunneling.

A schematic band diagram of charge tunneling through a TTEB SAM between a Au electrode and a Cu overlayer is shown in Figure 9.[18] A current of charge carriers tunneling through this system is made up either of electrons or of holes. Electrons tunnel through a barrier equal to the difference in energy between the TTEB lowest unoccupied molecular orbital (LUMO) and the Fermi energy of Cu. Holes tunnel through a different barrier with a height equal to the difference in energy between the TTEB HOMO and the Fermi energy of Au. The charge carrier tunneling through the smaller energy barrier will dominate the current. As the diagram shows, the barrier thickness remains equal to the thickness of the TTEB layer until the applied overpotential exceeds the barrier height. Once the applied potential exceeds the barrier height, the barrier thickness

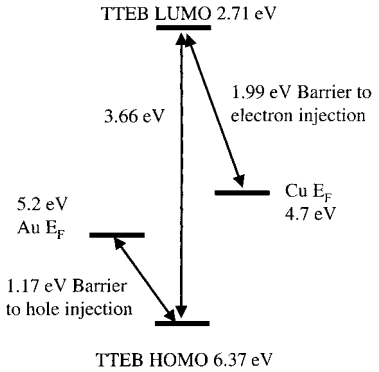

Figure 10. Schematic energy diagram illustrating the magnitude of energy barriers to electron/hole injection into TTEB from Au and Cu.

decreases with increasing voltage and tunneling enters the field-emission regime. This gives a crude measure of the barrier height as being comparable to the 1.1 V overpotential observed for Cu stripping on the ordered TTEB domains. The fact that this stripping occurs near the formal oxidation potential of TTEB further suggests that most of the charge is being carried by holes in this process.

A second estimate of the barrier height can be obtained from the relative energies of the TTEB HOMO, TTEB LUMO, Au Fermi, and Cu Fermi energies (Figure 10).[18] Electrochemistry gives the oxidation potential of TTEB as 1.4 V vs SCE, which is equal to 1.64 V vs the normal hydrogen electrode (NHE). The potential of the NHE has been measured at −4.73 V vs the vacuum electron energy;[19] therefore the energy of the HOMO may be estimated as 6.37 eV below the vacuum energy level. Holes travel from the Au Fermi energy at 5.2 eV into the HOMO through an estimated barrier height of 1.17 eV. The energy of the LUMO level may be estimated at 2.71 eV by combining the optically measured band gap, 3.66 eV, with the HOMO energy calculated above. The Fermi energy of Cu is 4.7 eV and results in a barrier to electron injection from Cu into the TTEB LUMO near 1.99 eV. Note, however, that the TTEB LUMO energy is only estimated by this method, since the corresponding reduction potential of TTEB cannot be observed within our solvent window. The smaller of these two estimated barriers to charge injection is the 1.17 eV barrier to hole injection, so we expect hole conduction to dominate. This value is consistent with the crude estimate of 1.1 V based on the observed overpotential given above.

Since the tunneling process is occurring in a field-emission regime (vide supra), Fowler−Nordheim tunneling analysis can also provide a measurement of the barrier height. Fowler and Nordheim derived the equations to describe charge carriers tunneling through triangular barriers.[20] They found that

$$I = F^2 e^{(-K/F)}$$

where I is the tunneling current, F is the electric field strength,

$$K = \frac{8\pi\sqrt{2M^*}\phi^{(3/2)}}{3qh}$$

M^* is the effective charge carrier mass, ϕ is the barrier height, q is the charge of the charge carrier, and h is Planck's constant. A plot of ln (I/F^2) vs $1/F$ gives a straight line with $-K$ as the slope from which the barrier height may be calculated.

The electrochemical data for the 1.2 V Cu oxidation peak in Figure 7 were transformed to tunneling current and electric field strength, required for a Fowler−Nordheim analysis. The observed current at 1.2 V comes from two sources. The first is

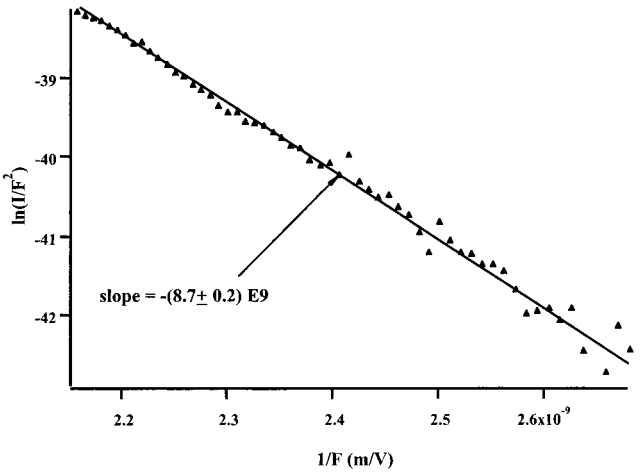

Figure 11. Fowler−Nordheim plot based on electrochemical data from Figure 7.

charge carriers tunneling between Au and Cu through TTEB, resulting in Cu oxidation, and the second is the capacitative charging of the electrode. Charging current is constant in linear sweep voltammetry and was estimated as the baseline current just prior to the tunneling peak. This baseline charging current was subtracted from the electrochemical current to give tunneling current. Field strength was calculated as the electrochemical overpotential divided by the thickness of the TTEB SAM, 25.2 Å.[2] The electrochemical overpotential for each point in the 1.2 V oxidation peak was determined by subtracting the potential of the Cu oxidation peak at SAM defect sites (0.012 V at the leading edge) from the electrochemical voltage. The Cu oxidation data for a Fowler−Nordheim analysis were selected from the leading edge of the 1.2 V oxidation in Figure 7. At lower potentials, nontunneling current dominates the observed electrochemical current. At more positive potentials, the loss of Cu from the electrode surface leads to lower observed currents because fewer TTEB molecules participate in conduction.

Figure 11 shows a Fowler−Nordheim plot based on data from Figure 7, including only data from the leading edge of the Cu oxidation peak. If the electric field strength is assumed to be constant through the TTEB SAM and the effective mass of an electron is approximated with the electron rest mass, the slope of this plot yields a tunneling barrier height through the TTEB SAM of 1.17 eV. This value is consistent with the two values calculated above by independent methods from these data.

Conclusions

The experiments reported here show that TTEB possesses a large energy barrier to the injection of charges from simple metal electrodes. The calculated barrier height of 1.17 eV is extremely large for a molecule intended to be a conductor. If we assume that every molecule beneath a Cu island is active, then rough estimation of the effective area of the islands suggests a current per active molecule less than 1 fA. This low value compared to STM measurements[4] on SAMs may be because not all molecules participate in conduction or perhaps may be due to differences in chemical and electronic nature between a STM tip and a planar Cu contact. Conversely, a molecule may be perturbed by the presence of a sharp metal tip, resulting in changes to its electronic structure. Any method that relies on a current feedback control loop to determine the position of a contact or the force applied to a sample could be susceptible to this problem.

Acknowledgment. We thank D. G. Dunkelberger for help with the SEM, T. Datta for allowing us to use the metal evaporation system, and the Office of Naval Research for support of this work under Grant N00014-97-1-0806.

References and Notes

(1) Jortner, J.; Ratner, M., Eds. *Molecular Electronics*; Blackwell Science: Malden, MA, 1997.

(2) Tour, J. M.; Jones, L.; Pearson, D. L.; Lamba, J. J. S.; Burgin, T. P.; Whitesides, G. M.; Allara, D. L.; Parikh, A. N.; Atre, S. V. *J. Am. Chem. Soc.* 1995, *117*, 9529.

(3) Tour, J. M.; Kozaki, M.; Seminario, J. M. *J. Am. Chem. Soc.* 1998, *120*, 8486.

(4) Bumm, L. A.; Arnold, J. J.; Cygan, M. T.; Dunbar, T. D.; Burgin, T. P.; Jones, L.; Allara, D. L.; Tour, J. M.; Weiss, P. S. *Science* 1996, *271*, 1705.

(5) Ulman, A. *An Introduction to Ultrathin Organic Films*; Academic: Boston, MA, 1991.

(6) Reed, M. A.; Zhou, C.; Muller, C. J.; Burgin, T. P.; Tour, J. M. *Science* 1997, *278*, 252.

(7) Van Patten, P. G.; Noll, J. D.; Myrick, M. L. *J. Phys. Chem*. 1996, *100*, 3646.

(8) Van Patten, P. G.; Noll, J. D.; Myrick, M. L. *Atomic Force Microscopy/Scanning Tunneling Microscopy 2*; Cohen, S. H., Lightbody, M. L., Eds.; Plenum: New York, 1997; pp 155−160.

(9) Van Patten, P. G. *Scanning Tunneling Microscopy Innovations for Chemical Synthesis and Analysis on the Nanometer Scale*; Dissertation, University of South Carolina, Columbia, SC, 1996.

(10) Van Patten, P. G.; Noll, J. D.; Myrick, M. L. *J. Vac. Sci. Technol. B* 1997, *15*, 282.

(11) Hawkes, P. W.; Kasper, E. *Principles of Electron Optics Vol. 2: Applied Geometrical Optics;* Academic: San Diego, CA, 1996; Chapter 44.

(12) Myrick, M. L.; Noll, J. D.; Nicholson, M. A. *J. Electrochem. Soc*. 1998, *145*, 179.

(13) Chen, J.; Reed, M. A.; Asplund, C. L.; Cassell, A. M.; Rawlett, A. M.; Van Patten, P. G.; Myrick, M. L.; Tour, J. M. *Appl. Phys. Lett.* 1999, *75*, 624.

(14) Wang, J. *Stripping Analysis: Principles, Instrumentation, and Applications*; VCH: Deerfield Beach, FL, 1991.

(15) Bard, A. J.; Faulkner, L. R. *Electrochemical Methods;* John Wiley & Sons: New York, 1980.

(16) Kissinger, P. T.; Heineman, W. R. *Laboratory Techniques in Electroanalytical Chemistry*, 2nd Ed; Marcel Dekker: New York, 1996.

(17) Finklea, H. O. *Electroanal. Chem*. 1996, *19*, 109.

(18) Parker, I. D. *J. Appl. Phys*. 1994, *75*, 1656.

(19) Gomer, R.; Tryson, G. *J. Chem. Phys*. 1977, *66*, 4413.

(20) Fowler, R. H.; Nordheim, L. *Proc. R. Soc. London, Ser. A* 1928, *119*, 173.